NeuroImage 123 (2015) 42–50

Contents lists available at ScienceDirect

NeuroImage

journal homepage: www.elsevier.com/locate/ynimg

Differential age-dependent associations of gray matter volume and white matter integrity with processing speed in healthy older adults

Zhaoping Hong [a], Kwun Kei Ng [a], Sam K.Y. Sim [a], Mei Yi Ngeow [a], Hui Zheng [a], June C. Lo [a], Michael W.L. Chee [a], Juan Zhou [a,b,*]

[a] Center for Cognitive Neuroscience, Neuroscience and Behavioral Disorders Program, Duke-National University of Singapore Graduate Medical School, Singapore
[b] Clinical Imaging Research Centre, the Agency for Science, Technology and Research and National University of Singapore, Singapore

ARTICLE INFO

Article history:
Received 30 May 2015
Accepted 16 August 2015
Available online 21 August 2015

ABSTRACT

Slower processing speed (PS), a highly robust feature of cognitive aging, is associated with white matter (WM) deterioration and gray matter volume (GMV) loss. Traditional linear regression models assume a constant relationship between brain structure and cognition over time. To probe for variation in the association between WM and GMV and PS over time, we used a novel sparse varying coefficient model on data collected from 126 relatively healthy older adults (67 females, aged 58–85 years) evaluated with MRI and a standardized neuropsychological test-battery. We found that WM microstructural differences indexed by fractional anisotropy values in the fronto-striatal tracts (internal and external capsule) showed a stronger association with PS before the age of 70 years. Contrastingly, GMV values of the left putamen and middle occipital gyrus were more strongly correlated with PS after 70 years. Additionally, within GM and WM compartments, there was heterogeneity in the temporal sequence in which different cortical and subcortical elements were most strongly associated with PS. Together, these observations provide a more nuanced account of the relationships between different structural components of the aging brain and processing speed, a key cognitive domain affected in relatively healthy older adults.

Introduction

Reduced processing speed (PS) is a highly robust feature of cognitive aging (Salthouse and Ferrer-Caja, 2003) that may underlie age-related decline in several higher order cognitive abilities (Salthouse, 1995, 2010). Tests of processing speed incorporate both elements of sensorimotor response time as well as the ability to rapidly switch between recently encountered item mappings. Reduced gray matter volume (GMV) and degraded white matter (WM) integrity have individually been shown to correlate with age-related reduction in PS (Fjell and Walhovd, 2010).

Reduced GMV could potentially contribute to slower PS by increasing noise in neuronal signals with resultant slowing of information processing. In a prior cross-sectional analysis of relatively healthy elderly participants (N = 248, aged 55–86 years), we found a correlation between total cerebral volume and PS. Lower GMV of the inferior frontal, superior parietal, and lingual gyri also correlated with slower PS (Chee et al., 2009). Another cross-sectional study of adults aged 19–79 years found that the particular spatial patterns of frontal and cerebellar gray and white matter were related to slower PS (Eckert et al., 2010). PS differences have also been associated with thinner medial frontal and occipito-temporal cortices (Righart et al., 2013).

White matter degradation could contribute to reduced PS in healthy aging by affecting the speed of information transfer throughout the brain (Bendlin et al., 2010; Charlton et al., 2006; Lu et al., 2011; Madden et al., 2012; O'Sullivan et al., 2001; Shenkin et al., 2005; Vernooij et al., 2009; Voineskos et al., 2012). DTI measures of WM microstructure are useful in measuring healthy and pathological aging (Fjell and Walhovd, 2010; Sullivan and Pfefferbaum, 2006). Fractional anisotropy (FA), a commonly reported diffusivity measure of WM integrity and efficiency, indexes the directional coherence of water displacement. A decrease in PS has been related to a reduction of FA mainly in the frontal-subcortical tracts including the genu of the corpus callosum (Bennett et al., 2012; Bucur et al., 2008; Haasz et al., 2013; Kennedy and Raz, 2009a; Salami et al., 2012; Zahr et al., 2009), anterior limb of internal capsule (ALIC) (Madden et al., 2004; Sullivan et al., 2010), external capsule (EC), superior longitudinal fasciculus, and inferior fronto-occipital fasciculus (Borghesani et al., 2013; Kerchner et al., 2012; Salami et al., 2012), and anterior corona radiata (ACR) (Mori et al., 2005; Wakana et al., 2004) in healthy older subjects. Based on a sample of very old adults (aged 81–103 years) assessed twice with an interval of 2.3 years, decreases in perceptual speed were associated with changes in WM integrity of the corticospinal tract over time (Lovden et al., 2014).

* Corresponding author at: Duke-NUS Graduate Medical School, 8 College Road, #06-15, Singapore 169857. Fax: 65 62218685.
E-mail address: helen.zhou@duke-nus.edu.sg (J. Zhou).

http://dx.doi.org/10.1016/j.neuroimage.2015.08.034
1053-8119/

These findings establish the individual contributions of GMV loss and WM integrity deterioration to reduced PS (Kennedy et al., 2009; Kennedy and Raz, 2009a; Madden et al., 2009; Pfefferbaum et al., 2000, 2005; Sullivan and Pfefferbaum, 2006). However, it remains unclear as to how they jointly contribute to PS slowing as aging progresses (Fjell and Walhovd, 2010; Madden et al., 2009). Structural equation modeling has been applied to investigate how age and WM integrity influence cognitive performance in healthy subjects across the lifespan (Voineskos et al., 2012). Along similar lines, mediation analysis has been used to demonstrate how loss of WM integrity (FA) can mediate the relationship between age and PS (Kerchner et al., 2012). However, mediation models used in cross-sectional data may be biased (Lindenberger et al., 2011; Maxwell and Cole, 2007).

In contrast to the prevailing assumption that the contribution of a given brain structure to cognitive decline is constant over time, recent large-scale studies have identified nonlinear trajectories of age-related decreases in brain structural integrity (Ostby et al., 2009). A range of linear, quadratic, and cubic correlations between age and cortical thickness has been identified in different brain regions (Shaw et al., 2008; Sowell et al., 2003). Across the lifespan, the trajectories of GM and WM maturational and aging effects vary considerably across the cortex. Widespread reductions in GMV that are observed from middle age onward are preceded by changes restricted to the frontal cortex (Giorgio et al., 2010). In contrast, widespread WM microstructure changes are found from young adulthood onward, each white matter region exhibiting different linear or nonlinear lifespan trajectories (Giorgio et al., 2010; Kennedy and Raz, 2009b; Westlye et al., 2010). Indeed, initial decline in white matter integrity can begin as early as 23 years of age (Imperati et al., 2011), raising the possibility that WM degradation may exert a stronger influence on cognitive performance earlier in age than declines in GM volume.

In light of these prior findings, we examined the differential age-dependent associations of regional WM FA and GMV with PS using the sparse varying coefficient (SVC) model (Daye et al., 2012). Unlike linear models used in previous studies, the SVC model does not assume constant association between a brain structure and PS across age, instead allowing for the association to vary with age. We hypothesized that (1) age-related reductions in the WM FA and GMV mainly within the fronto-striatal circuits and sensory cortices would be associated with slower PS and (2) the strength of the associations would not remain constant over time but instead vary with age. Specifically, based on prior evidence that WM microstructure metrics might decline earlier than GMV in aging, we expected deterioration in FA to correlate with PS earlier than GMV loss.

Methods

Participants

The participants were from the Singapore Longitudinal Aging Brain Study (Chee et al., 2009), a community-based convenience sample cohort comprising relatively healthy elderly adults. The current sample consisted of 126 participants (67 females, aged 58–85 years, all right-handed, age distribution in Supplementary Fig. 1B) who underwent both neuropsychological assessments and quality-controlled MRI and DTI scans during 2009–2010. They were of Han Chinese ethnicity and had no known active medical conditions other than treated, uncomplicated diabetes mellitus or hypertension (Table 1). They did not have any of the following: (1) a history of significant vascular events (i.e., myocardial infarction, stroke, or peripheral vascular disease); (2) a history of malignant neoplasia of any form; 3) a history of cardiac, lung, liver, or kidney failure; (4) active or inadequately treated thyroid disease; (5) active neurological or psychiatric conditions; (6) a history of head trauma with loss of consciousness; (7) a Mini Mental State Examination (MMSE) (Folstein et al., 1975) score of less than 26; or (8) a 15-point modified-Geriatric Depression Screening Scale (GDS) (Sheikh and Yesavage, 1986) score of greater than 9. The Institutional Review Board at the National University of Singapore granted approval for this study. All participants provided written informed consent prior to participation.

Table 1
Subject characteristics (N = 126).

Variables	Mean (SD)
Age (years)	69.3 (6.5)
Number of females	67
Education (years)	11.9 (3.4)
BMI (weight kg / height m^2)	23.4 (2.9)
Systolic blood pressure (mm Hg)	138.2 (16.9)
Diastolic blood pressure (mm Hg)	73.9 (9.9)
Mini Mental State Examination	28.2 (1.3)
Trail-Making Test A (seconds)	41.6 (14.9)
Symbol–Digit Modalities Test Written	44.3 (10.6)
Symbol–Digit Modalities Test Oral	51.1 (10.4)
Symbol search	27.3 (8.0)

Abbreviation: BMI = body mass index.

Neuropsychological assessments

Within 3 months of undergoing MR imaging, all participants underwent a comprehensive neuropsychological assessment that evaluated six cognitive domains: PS, attention, verbal memory, visuospatial memory, executive functioning, and language. To minimize the effects of language and culture, the included tests contained items that were relatively familiar to the study population (Chee et al., 2009). Here, we assessed PS using the Trail-Making Test A (Reitan and Wolfson, 1985), the Symbol–Digit Modalities Test (SDMT) (Smith, 1991), and symbol search test (Wechsler, 1997). The Trail-Making Test A recorded the time to complete the connection of 25 circles that contained numbers in an ascending order. The time in seconds was then multiplied by −1 to enable a higher score to indicate better performance. The SDMT required the participants to substitute a number for its corresponding geometric figure in both written and oral formats, with each format lasting 90 seconds. The raw score was the total number of correct answers. The symbol search test lasted for 120 seconds and required the participants to decide whether the target symbol appeared in a row of symbols. The raw score was the total number of correct answers. The raw scores of these three tests were normalized into *z*-scores across 126 participants. We generated one composite score for PS per participant by taking the average of the three *z*-scores to reduce the number of comparisons.

Image acquisition

MRI scans were conducted on a 3 T Siemens Magnetom Tim Trio System (Siemens, Erlangen, Germany). All 126 participants had DTI acquisition using a diffusion-weighted echo-planar imaging (EPI) sequence (30 non-collinear diffusion gradient directions at b = 1000 seconds/mm^2, six volumes of b = 0 seconds/mm^2, TR/TE = 9600/107 ms, FOV = 256 × 256 mm^2, matrix = 128 × 128, 54 contiguous slices, and voxel size = 2.0 × 2.0 × 2.0 mm^3). High-resolution T1-weighted structural MRI was acquired using MPRAGE (magnetization-prepared rapid gradient echo) sequence (192 continuous sagittal slices, TR/TE/TI = 2300/2.98/900 ms, flip angle = 9°, FOV = 256 × 240 mm^2, matrix = 256 × 256, isotropic voxel size = 1.0 × 1.0 × 1.0 mm^3, bandwidth = 240 Hz/pixel) for 119 participants and MEMPRAGE (multi-echo MPRAGE) (192 continuous sagittal slices, TR/TE/TI = 2530/2.98/1200 ms, flip angle = 7°, FOV = 256 × 256 mm^2, matrix = 256 × 256, isotropic voxel size = 1.0 × 1.0 × 1.0 mm^3, bandwidth = 651 Hz/pixel) for the remaining 7 participants.

Tract-based spatial statistics: FA and processing speed

The DTI data were preprocessed using FSL (http://www.fmrib.ox.ac.uk/fsl). Following our previous approach (Cortese et al., 2013), eddy current distortion and head movement were corrected through affine registration of diffusion-weighted images to the first b = 0 volume. Data were discarded if the maximum displacement relative to the first b = 0 volume was more than 3 mm. Diffusion gradients were rotated to improve consistency with the motion parameters. FA images were created by fitting a diffusion tensor model to the diffusion data at each voxel. We then applied tract-based spatial statistics (TBSS) (Smith et al., 2006) to carry out a voxel-wise analysis of FA data within major WM pathways throughout the whole brain. The FA images of all participants were first registered to FMRIB58_FA standard space image with 1 mm^3 resolution using the nonlinear registration tool FNIRT (Andersson et al., 2007). The TBSS minimizes the problem of intersubject registration by first determining a mean FA skeleton (thresholded at 0.25), representing only the center of major WM fiber tracts. Each participant's aligned FA data were then projected onto this skeleton, resulting in subject-level skeletonized FA images.

To examine the relationship between WM FA and PS in 126 healthy older adults, we built voxel-wise general linear models (GLM) with the skeletonized WM FA images as the dependent variable, PS as the covariate of interest, and gender as the nuisance variable (Fig. 1, step 1). The WM regions where the skeletonized FA was positively correlated with PS were identified using permutation-based non-parametric testing (FSL RANDOMISE), thresholded at $p < 0.05$ with threshold-free cluster enhancement (TFCE) correction (Smith and Nichols, 2009). Anatomical localization of the identified WM clusters was determined with reference to the Johns Hopkins University white matter atlas labels (Mori et al., 2005). The subject-level mean FA values of each identified WM tracts were computed for further statistical analyses.

Voxel-based morphometry: GMV and processing speed

We applied an optimized voxel-based morphometry (VBM) protocol (Good et al., 2001) using Statistical Parametric Mapping (SPM8) (http://www.fil.ion.ucl.ac.uk/spm/). We derived the subject-level GMV probability maps from T1 structural images following our previous approach (Zhou et al., 2010), including (1) segmented individual T1-weighed images into GM, WM, and cerebrospinal fluid (CSF); (2) created a study-specific template using nonlinear DARTEL registration (Ashburner, 2007); (3) registered each GM/WM probability maps to the customized template in MNI space and performed tissue segmentation; (4) performed modulation by multiplying voxel values by the Jacobian determinants derived from the spatial normalization step; (5) applied smoothing on the normalized GM maps by a 10 mm isotropic Gaussian kernel. GMV of each participant was normalized (divided by total estimated intracranial volume (eTIV)) for further statistical analyses.

To examine the association between GMV and PS in 126 healthy older adults, the subject-level GMV probabilistic maps were entered into a general linear model with PS as the covariate of interest, and gender and type of T1-weighted image sequence as the nuisance covariates (Fig. 1, step 1). The GM regions where the GMV was positively correlated with PS were identified at $p < 0.001$ uncorrected with a cluster size threshold of 160 voxels. The cluster extent threshold was determined based on the expected number of voxels per cluster according to random field theory implemented in SPM (Hayasaka and Nichols, 2004). The mean volume of the identified GM regions was calculated for each participant for further statistical analyses.

Statistical analyses

From the set of brain areas derived from step 1 where the WM FA had a positive correlation with PS, we subsequently examined whether the FA and age contributed to PS independently. For each candidate brain region, we performed a hierarchical regression analysis that compared the associations of age and cluster-wise mean FA with PS across all participants (Fig. 1, step 2). Age was first entered into the model followed by FA, with gender as a nuisance variable. The changes in R^2 after adding FA to the model were determined, and the beta values of FA and age were compared. The same approach was used to determine whether the GMV of the identified regions (from step 1) remained a predictor of PS after accounting for age (Fig. 1, step 2). To control for the contribution of education, we repeated the above hierarchical regression analyses with years of education as a nuisance variable.

Finally, rather than assuming independent contribution of age and brain structure to PS in normal aging, we aimed to test whether and how the associations of brain structures with PS were modulated by

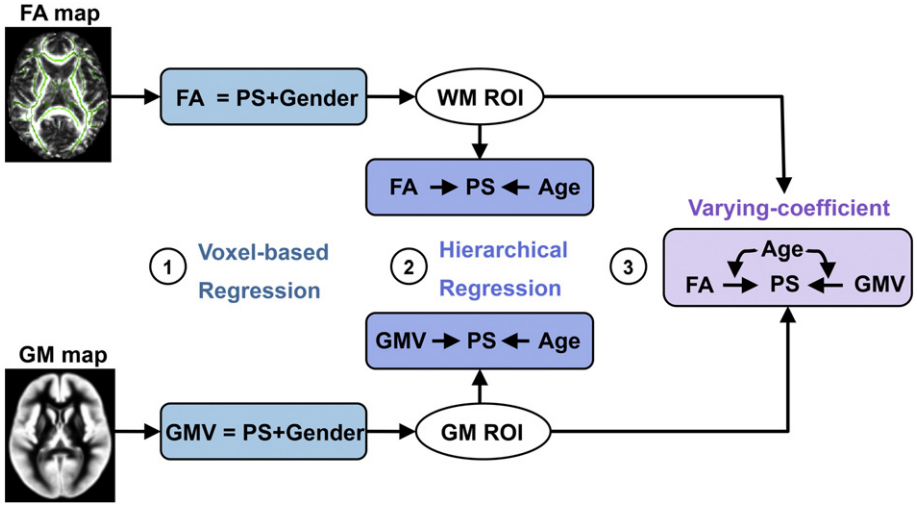

Fig. 1. *Study design schematic.* The study included three steps: (1) whole-brain voxel-based linear regressions were performed on fractional anisotropy (FA) maps and probabilistic gray matter volume (GMV) maps against processing speed (PS) composite scores in 126 healthy older adults; (2) for each candidate region of interest derived from step 1, the differential associations of FA/GMV and age with PS were compared using hierarchical regression; (3) from the sets of candidate regions of interest, a sparse varying coefficient model was built to select the regions where WM FA or GMV act as key predictors of PS while simultaneously estimating how these predictors were associated with PS in an age-dependent manner.

age. To achieve this goal, we proposed using an SVC model (Daye et al., 2012) with PS as the dependent variable (Fig. 1, step 3):

$$y_i(t_k) = \sum_{j=1}^{p} \beta_j(t_k) x_{ij}(t_k) + \varepsilon_i(t_k),$$

where $y_i(t_k)$ was the PS score for subject $i(i = 1,2,\ldots,n)$ at age t_k ($k = 1,2,\ldots,K$), $x_{ij}(t_k)$ was the j^{th} ($j = 1,2,\ldots,p$) predictor (including brain structure measures and nuisance variables, such as gender and type of T1-weighted image) of subject i at age t_k, $\beta_j(t_k)$ was the coefficient function depending on age t_k for each feature j and $\varepsilon_i(t_k)$ were the independent and identically distributed random errors at t_k. We approximated each coefficient function β_j using linear combinations of the B-spline basis. To simultaneously achieve the regression model fitting and variable selection, we applied the least absolute shrinkage and selection operator (LASSO) (Tibshirani, 1996) to estimate $\beta_j(t_k)$ by minimizing the following penalized least squares function:

$$\frac{1}{2n}\sum_{i=1}^{n}\sum_{k=1}^{K}\left[y_i(t_k) - \sum_{j=1}^{p} x_{ij}(t_k)\beta_j(t_k)\right]^2 + \lambda\sum_{j=1}^{p}\sqrt{\int \beta_j^2(t)dt},$$

where λ is the sparse penalty tuning parameter, which was chosen by a five-fold cross-validation method. The LASSO algorithm performs variable selection by constraining the sum of the magnitudes of the coefficient. SVC modeling with LASSO algorithm was specifically designed for feature selection problem with small sample size (Daye et al., 2012).

Our model offers three advantages over a traditional linear regression model: (1) it does not assume that the association of a brain structure with PS remains constant over time, thus, the SVC model considers each beta coefficient (the association of brain structure with PS) as a nonlinear function of age; (2) rather than analyzing WM or GM measures in separate models, WM FA and GMV variables (the variables that exhibited significant positive correlations with PS derived from step 1) are entered as predictors in the same multivariate model; and (3) feature selection with the LASSO sparse penalty chooses the most important predictors while eliminating the contribution of the less important predictors. As a result, we built one SVC model to identify specific brain structural measures (GMV and FA) from a group of candidates identified in step 1 as key predictors of PS in a group of older adults. Gender, eTIV, and type of T1-weighted image were included as the nuisance variables. We report the brain structural measures that were selected in all 100 repetitions of SVC modeling. The resulting SVC model identified a set of critical brain structural measures (FA/GMV) that contributed to PS as a result of age. The contribution of each independent variable to PS as a function of age was indicated by a vector of non-zero beta coefficients. To assess the stability of these beta coefficients, we calculated the mean and standard error of the age-dependent coefficients estimated from 100 replicates. Moreover, to assess the specificity of SVC modeling for our data, we randomly permuted the PS scores 100 times across the subjects and repeated the SVC modeling 100 times on each of the 100 permuted data sets. In addition, we ran the SVC modeling with gender, eTIV, type of T1-weighted image, and years of education (see Supplementary Materials for more details on SVC model implementation).

To assess whether WM integrity measured by another metric mean diffusivity (MD) was also associated with PS in an age-dependent manner, we first extracted mean MD values of the WM clusters derived from step 1 where the WM FA had a positive correlation with PS. Then we repeated the SVC modeling for MD and GMV (see Supplementary Materials).

Results

Associations of fractional anisotropy with processing speed

There was a significant negative correlation between age and PS ($r = -0.53$, $p = 2.6 \times 10^{-10}$, Supplementary Fig. 1A). The voxel-wise GLM (Fig. 1, step 1) revealed that the FA values in 35 WM regions were positively correlated with PS ($p < 0.05$, TFCE corrected) (Fig. 2, Supplementary Table 1), including the frontal WM (anterior corona radiata (ACR)), genu and body of the corpus callosum (CC), internal capsule, superior frontal WM (superior corona radiata (SCR)), temporal WM, splenium of the CC, and occipital WM areas. No WM cluster exhibited a negative correlation with PS. Moreover, there was a significant but weaker negative correlation between age and other four cognitive domains: executive function ($r = -0.38$, $p = 7.0 \times 10^{-6}$), verbal memory ($r = -0.24$, $p = 5.5 \times 10^{-3}$), visuospatial memory($r = -0.239$, $p = 6.9 \times 10^{-3}$), and language ($r = -0.21$, $p = 0.02$). The correlation

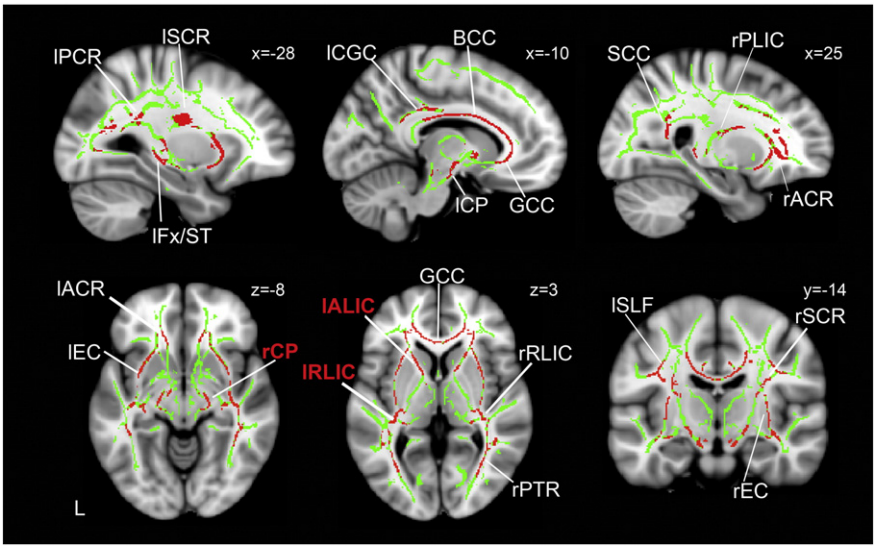

Fig. 2. *White matter regions where fractional anisotropy (FA) exhibited a significant positive correlation with the processing speed (PS).* Regions highlighted in red represent the WM clusters where FA was positively correlated with PS (thresholding at $p < 0.05$, TFCE corrected). The regions in green represent the mean FA skeleton generated for all participants. The WM clusters whose names are highlighted in red significantly contributed to PS after accounting for age (hierarchical regression analysis). PCR = posterior corona radiate; SCR = superior corona radiate; Fx/ST = fornix/stria terminalis; CGC = cingulum (cingulate gyrus); GCC = genu of the corpus callosum; BCC = body of the corpus callosum; CP = cerebral peduncle; SCC = splenium of the corpus callosum; PLIC = posterior limb of the internal capsule; ACR = anterior corona radiate; EC = external capsule; RLIC = retrolenticular part of the internal capsule; ALIC = anterior limb of the internal capsule; PTR = posterior thalamic radiation (include optic radiation); SLF = superior longitudinal fasciculus; r = right; and l = left.

between age and attention was not significant ($r = -0.15$, $p = 0.09$). TBSS analysis revealed that there was no WM region whose FA values had significant associations with these five cognitive domains ($p < 0.05$, TFCE corrected).

To determine whether FA predicts PS independent of age, we built hierarchical regression models of PS on age in each of the 35 WM tracts (Fig. 1, step 2, Supplementary Table 2). For 3 of these 35 regions, R^2 of PS significantly increased when FA was entered into the model (thresholded at $p < 0.05$ Bonferroni correction for multiple comparisons, Fig. 2, the name of tracts highlighted in red). These three regions were the left anterior limb of the internal capsule (ALIC), left retrolenticular part of the internal capsule (RLIC), and right cerebral peduncle (Supplementary Table 2). By comparing the beta coefficients of FA and age, the association of age with PS was stronger than that of the FA values in all 35 regions. When education was added into the hierarchical regression model, significant R^2 increase was found only for the left ALIC (Supplementary Table 3).

Associations of gray matter volume with processing speed

The voxel-wise GLM analysis of the GMV and PS (Fig. 1, step 1) yielded 7 clusters where the GMV was positively correlated with PS, including the bilateral putamen (PUT), bilateral precentral gyrus/paracentral lobule, left middle occipital gyrus (MOG), and right calcarine (CAL) (uncorrected $p < 0.001$ and cluster size > 160) (Fig. 3 and Supplementary Table 4). There was no GM region where the GMV was negatively correlated with PS.

To determine whether GMV remained significantly associated with PS after accounting for age, we built hierarchical regression models of PS on age and the volume of each of the 7 GM regions (Fig. 1, step 2, Supplementary Table 5). For 2 of these GM regions (left MOG and right CAL), R^2 of PS increased significantly when their volume was entered into the model (thresholded at $p < 0.05$, Bonferroni correction for multiple comparisons, Fig. 3, the name of regions highlighted in blue, Supplementary Table 5) while left PUT and right precentral gyrus/paracentral lobule was significant at $p < 0.05$ uncorrected. By comparing the beta coefficients of GMV and age, the effect of age on PS was larger than GMV in all 7 regions. With education as additional nuisance variable in the hierarchical regression model, significant R^2 increase was observed when GMV of the same four regions was entered into the model (Supplementary Table 6).

Age-dependent associations of FA and GMV with processing speed

To investigate the age-dependent contributions of both WM FA and GMV on PS, we built an SVC model with PS as the dependent variable and all 35 WM ROIs and 7 GM ROIs derived from step 1 as predictors (Fig. 1, step 3). We found that the FA of 6 WM tracts (the left ALIC, left RLIC, left ACR, right SCR, left external capsule (EC), and left fornix/stria terminalis (Fx/ST)), as well as the GMV of 2 GM regions (the left PUT and left MOG), were critical predictors of PS (Fig. 4, row 1). Each brain structural measure exhibited specific age-dependent associations with PS (Fig. 4, rows 2 and 3). By examining the amplitude of the beta coefficients of FA and GMV, the left PUT (GMV), left MOG (GMV), and left ALIC (FA) had the largest associations with PS. When the years of education was added into the SVC modeling as a covariate, FA of 4 WM tracts (the left ALIC, left ACR, right SCR, and left Fx/ST), as well as the GMV of 2 GM regions (the left PUT and left MOG) and years of education were selected as critical predictors of PS (Supplementary Fig. 2). The estimated age-dependent relationships of most regions remained the same as the SVC model without education.

We applied the SVC model on 100 permuted data sets to evaluate the specificity of our results. For 50 out of the 100 permuted data sets, no variable was selected by all 100 repetitions. For each of the remaining 50 permutated data sets, the SVC model selected one variable from 44 predictors as the key predictor of PS based on 100 repetitions. However, the frequency distribution of variable selection across these 50 data sets was approximately random (Supplementary Fig. 3). The 8 selected variables based on our original data were not favored over other variables in the null distribution. This indicates that the SVC model built on the original data set had high specificity.

Importantly, we found that the associations of WM FA and GMV with PS had distinct age-related trajectories (Fig. 4). Specifically, the association of FA in the WM tracts next to the putamen (left ALIC and left EC) with PS started in the early 60s, reached a maximum in the early 70s and then decreased, while the association of the GMV of the left PUT (surrounded by the two WM tracts) only began to appear at approximately 70 years of age and continued to increase thereafter. Similarly, the association of the WM FA in the left RLIC (which links the thalamus to the visual cortex) with PS preceded the effect of GMV of the left MOG. The association of FA (in the right SCR, left ACR, and left Fx/ST) or GMV (of the left MOG) started earlier than the association within the subcortical regions (FA in the left ALIC, EC, and PLIC and GMV of the left PUT). Similar analyses on MD yielded qualitatively consistent age-related associations of WM-preceding-GMV alternations with PS (see Supplementary Materials).

Discussion

The present results provide new insight into age-dependent associations between various measures of brain structure/integrity and PS in relatively healthy older adults. As expected, PS was lower among older participants (Cerella and Hale, 1994; Salthouse, 2000, 2009). A traditional hierarchical regression confirmed that FA and GMV were correlated with PS, though the associations were partially accounted for by age. Instead of assuming a constant association of brain structure with PS across age, we built a novel SVC model based on both WM FA and GMV measures. The association between WM FA and PS dominated

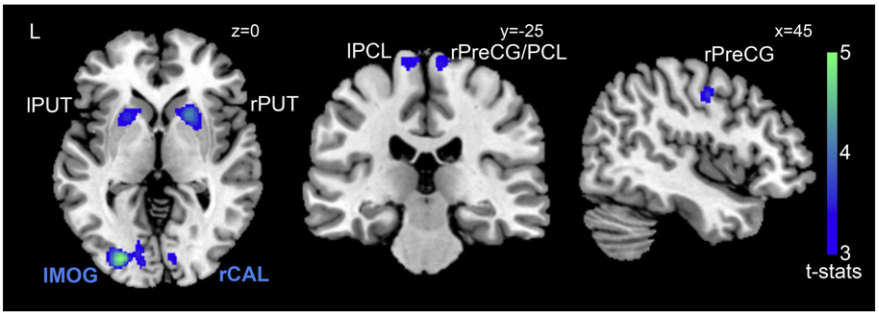

Fig. 3. *Brain regions where the gray matter volume (GMV) had a significant positive correlation with the processing speed (PS).* Regions highlighted in blue represent the GM clusters where the GMV was positively correlated with PS (uncorrected $p < 0.001$ and cluster size > 160 voxels). The GM brain regions whose names are highlighted in blue had significant contribution to PS after accounting for age (hierarchical regression analysis). PUT = putamen; MOG = middle occipital gyrus; CAL = calcarine; PCL = paracentral lobule; PreCG = precentral gyrus; r = right; and l = left.

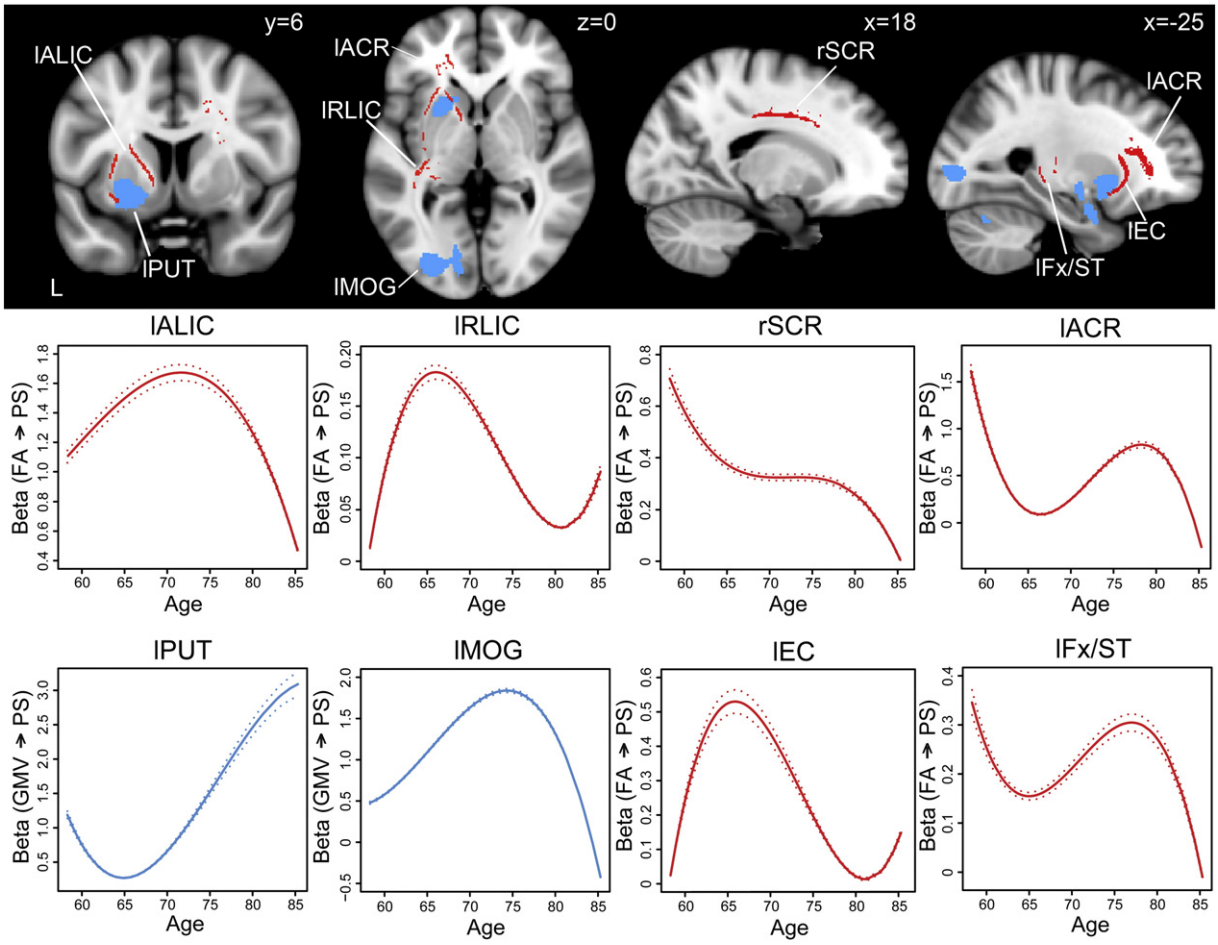

Fig. 4. *The age-dependent associations of white matter (WM) fractional anisotropy (FA) and gray matter volume (GMV) with processing speed (PS) derived from a sparse varying coefficient model.* Row 1: Spatial maps depict the brain regions where WM FA (red) and GMV (blue) were selected as predictors of PS. Rows 2 and 3: Solid curves represent the mean correlations of FA (red) or GMV (blue) with PS as a function of age estimated from 100 replicates. The dashed lines represent the point-wise 2* standard error of the solid curves estimated from 100 replicates. Abbreviations: SCR = superior corona radiate; Fx/ST = fornix/stria terminalis; ACR = anterior corona radiate; EC = external capsule; RLIC = retrolenticular part of the internal capsule; ALIC = anterior limb of the internal capsule; PUT = putamen; MOG = middle occipital gyrus; r = right; and l = left.

before the age of 70 years while the GMV was more strongly associated with reduced PS after that. These findings provide support for age-dependent trajectories in associations between brain structure and PS.

FA and GMV: Differential age-dependent associations with processing speed

Previous studies have focused on the relationships between either diffusion characteristics or gray matter features with the aging brain, and studies evaluating their effects in combination are rare (Abe et al., 2008). Additionally, the association between brain structure and cognitive functioning may change with aging (Salthouse, 2011). Using mediation analyses, Kerchner and colleagues found that the relationship between age and reaction time might be mediated by FA (Kerchner et al., 2012). Age-related FA differences (mainly in the external capsule and body of the corpus callosum) mediated, in part, the age-related decline in PS but not that of other cognitive domains, such as episodic memory or visuospatial ability (Salami et al., 2012).

By examining region-specific GMV and WM FA together in one SVC model, we found that WM FA (left ALIC, left EC, and left RLIC) were associated with PS at an earlier age than GMV of nearby regions (left PUT and left MOG). Our findings suggest that reduced integrity of subcortical WM tracts, i.e., demyelination and axonal damage, might be associated with age-related slowing in PS, and these relationships precede those of GMV loss within the related regions. This finding is consistent with the observation that degradation of WM microstructure observed from young adulthood onward (Giorgio et al., 2010; Imperati et al., 2011; Kochunov et al., 2011; Westlye et al., 2010) largely precedes widespread changes in the GMV (from middle age onward).

The age-dependent associations of GMV and WM FA on PS exhibited cortical and subcortical heterogeneity. The association of the subcortical GMV with PS started later than the GMV of the left MOG. In contrast, the magnitude of association of the former became greater than that of the MOG after 75 years of age. This finding is consistent with the finding of greater aging-related GMV loss in the cortex than in subcortical structures (Jernigan et al., 2001; Walhovd et al., 2005, 2011). Along similar lines, subcortical tracts (left EC, ALIC, and RLIC) correlate more strongly with PS at a later age than cortical or limbic WM tracts (right SCR, left ACR, and left Fx/ST). Both the internal and external capsules are early maturing tracts that exhibit slower aging (changes in FA/year) compared with the late maturing cortical WM tracts (Kochunov et al., 2011). Previous lifespan trajectory studies have demonstrated that FA exhibits an inverted-U relationship with age. Interestingly, internal and external capsules begin to degenerate at approximately 30–34 years of age, while cortical FA values in the ACR, SCR, and Fx/ST begin to decline at approximately 23–26 years of age (Imperati et al., 2011; Lebel et al., 2012). Taken together, it appears that cortical WM tracts, including the left ACR (which links the frontal lobe to the putamen and thalamus), the right SCR (an extension of the internal capsule), and the left Fx/ST (which links the hippocampus to the hypothalamus) (Giorgio et al., 2010), might deteriorate before the subcortical external and internal capsules. These differential age-dependent structural

changes in cortical and subcortical regions might explain their heterogeneous associations with PS.

Associations of cortical-striatal circuits with processing speed

By allowing the association of structural integrity with PS to vary with age and simultaneously considering GMV and FA, our SVC model suggests that the GMV of the left MOG and left putamen are key age-dependent correlates of slower PS. Consistent with previous findings (Zhang et al., 2011), the association of volume loss within the visual cortex (left MOG) with slower PS suggests age-related decreases in visual processing speed. There is little doubt that the putamen is critical for motor execution and motor learning (DeLong et al., 1984; Marchand et al., 2008; Turner et al., 2003). Recent findings, however, have suggested that the putamen plays a key role in all functionally defined cortico-striatal loops (affective, cognitive, and sensorimotor) (Alexander et al., 1986; Haber, 2010). The putamen is in a position to participate in information processing within, and perhaps across, cortico-striatal loops (Ell et al., 2011). Particularly, fMRI studies have demonstrated that activations in the striatum (putamen and caudate nucleus) are uniquely associated with encoding time intervals for information processing (Rao et al., 2001; Schubotz et al., 2000). The putamen is a brain structure that shows highly consistent age-related decline in volume (Fjell and Walhovd, 2010; Kalpouzos et al., 2009; Walhovd et al., 2005). This could plausibly degrade the neural representation and impair the recognition of stimuli and information integration within and across the cortico-striatal loops. For example, putamen atrophy predicted slower auditory and visual information PS using the paced auditory serial addition test and the symbol digit modality test in patients with multiple sclerosis (Batista et al., 2012).

Strikingly, one recent study has demonstrated that PS correlated strongly with the fiber connections between the putamen and the visual and lingual cortices, as well as the fiber connections between the putamen and the motor cortex in normal aging (Ystad et al., 2011). Here, we identified fronto-striatal FA as a key predictor of the age-related differences in PS. Age-related degradation in WM (e.g., demyelination or axonal loss) may affect communication between distributed GM regions within a neural network (Andrews-Hanna et al., 2007; Sullivan and Pfefferbaum, 2006). The ALIC and EC form a critical part of the fronto-striatal connections between deep GM structures and the frontal cortex. Madden and colleagues demonstrated that FA in the ALIC was a good predictor of response time in a visual target-detection task among older adults (Madden et al., 2004). Further, FA in the EC may contribute to letter digit substitution task performance (Salami et al., 2012). WM FA in the left ACR and right SCR have been associated with performance in the Trail-Making Test A among older adults (Jacobs et al., 2013). PS has been correlated with FA values in the Fx/ST to promote effective and efficient performance (Zahr et al., 2009). In sum, it appears that there is a clear association between a combination of gray matter loss (neuronal representation) and degradation of white matter integrity (communications) within cortico-striatal circuits and slower PS in relatively healthy older adults.

Conclusions and limitations

Several limitations of the current study should be acknowledged. First, this is a cross-sectional study. Therefore, the associations between brain structure and PS derived by the statistical model are simply age-dependent correlations and need to be interpreted with caution. Hierarchical regression showed that most of the structural associations with PS are not independent of age. On the other hand, whether a predictor is independent of age or not is not a critical feature for understanding the role of that predictor in the age-dependent correlations (Hayes, 2009). Such age-dependent associations between brain structure and PS remain to be tested in longitudinal data sets. Second, the age distribution of the participants was not uniform; there were a limited number of participants aged 58–59 and 80–85 years. This uneven distribution might affect the estimation accuracy in the SVC modeling at the two ends of the age spectrum. Including young and middle-aged participants in the study would have produced a more complete picture of the age-associated associations on brain structure and PS. Moreover, we employed a TBSS method to extract and project FA to a group-based WM fiber skeleton. Although TBSS partially overcomes the misalignment of FA images in a WM voxel-based analysis (VBA) (Smith et al., 2006), altered WM near the boundary of WM and GM may be less accurately captured. Similarly, the observed gray matter volume differences derived from VBM might be confounded by inaccurate tissue segmentation or registration (Kennedy et al., 2009). Fourth, when investigating the relationships between brain structural measures and cognition, one common question is whether age-related differences in individual brain regions can be interpreted independently of more global, whole-brain age effects. The traditional approach of analyzing individual regions/tracts separately did not take into account the shared variance across regions (Bennett and Madden, 2014). However, it is unlikely that our findings were the results of a non-specific global effect because the model used to predict the PS reduction considers the FA values of multiple tracts and the GMV of multiple regions, as well as the eTIV, simultaneously.

In summary, we demonstrated that the trajectories of associations between brain structure (WM FA and GMV) and PS differ: WM microstructural deterioration preceded GMV loss in spatially related regions. In addition, there is cortical–subcortical heterogeneity in the temporal sequence of associations with PS. The application of the SVC model to simultaneously model the age-dependent associations of region-specific GMV and WM FA with PS provide incremental insight into the neurobiological mechanisms underlying cognitive aging.

Disclosure statement

The authors have no potential conflicts of interest.

Acknowledgments

We would like to thank all subjects for their participation in this study. This research was supported by the Biomedical Research Council, Singapore: BMRC 04/1/36/372, the Agency for Science, Technology, and Research (A*STAR) and Duke-NUS Graduate Medical School Signature Research Program funded by Ministry of Health, Singapore.

Appendix A. Supplementary data

Supplementary data to this article can be found online at http://dx.doi.org/10.1016/j.neuroimage.2015.08.034.

References

Abe, O., Yamasue, H., Aoki, S., Suga, M., Yamada, H., Kasai, K., Masutani, Y., Kato, N., Kato, N., Ohtomo, K., 2008. Aging in the CNS: comparison of gray/white matter volume and diffusion tensor data. Neurobiol. Aging 29, 102–116.

Alexander, G.E., DeLong, M.R., Strick, P.L., 1986. Parallel organization of functionally segregated circuits linking basal ganglia and cortex. Annu. Rev. Neurosci. 9, 357–381.

Andersson, J.L.R., Jenkinson, M., Smith, S.M., 2007. Non-linear registration, aka spatial normalisation. FMRIB technical report TR07JA2.

Andrews-Hanna, J.R., Snyder, A.Z., Vincent, J.L., Lustig, C., Head, D., Raichle, M.E., Buckner, R.L., 2007. Disruption of large-scale brain systems in advanced aging. Neuron 56, 924–935.

Ashburner, J., 2007. A fast diffeomorphic image registration algorithm. NeuroImage 38, 95–113.

Batista, S., Zivadinov, R., Hoogs, M., Bergsland, N., Heininen-Brown, M., Dwyer, M.G., Weinstock-Guttman, B., Benedict, R.H., 2012. Basal ganglia, thalamus and neocortical atrophy predicting slowed cognitive processing in multiple sclerosis. J. Neurol. 259, 139–146.

Bendlin, B.B., Fitzgerald, M.E., Ries, M.L., Xu, G., Kastman, E.K., Thiel, B.W., Rowley, H.A., Lazar, M., Alexander, A.L., Johnson, S.C., 2010. White matter in aging and cognition: a cross-sectional study of microstructure in adults aged eighteen to eighty-three. Dev. Neuropsychol. 35, 257–277.

Bennett, I.J., Madden, D.J., 2014. Disconnected aging: cerebral white matter integrity and age-related differences in cognition. Neuroscience 276, 187–205.
Bennett, I.J., Motes, M.A., Rao, N.K., Rypma, B., 2012. White matter tract integrity predicts visual search performance in young and older adults. Neurobiol. Aging 33, 433, e421–431.
Borghesani, P.R., Madhyastha, T.M., Aylward, E.H., Reiter, M.A., Swarny, B.R., Schaie, K.W., Willis, S.L., 2013. The association between higher order abilities, processing speed, and age are variably mediated by white matter integrity during typical aging. Neuropsychologia 51, 1435–1444.
Bucur, B., Madden, D.J., Spaniol, J., Provenzale, J.M., Cabeza, R., White, L.E., Huettel, S.A., 2008. Age-related slowing of memory retrieval: contributions of perceptual speed and cerebral white matter integrity. Neurobiol. Aging 29, 1070–1079.
Cerella, J., Hale, S., 1994. The rise and fall in information-processing rates over the life span. Acta Psychol. 86, 109–197.
Charlton, R., Barrick, T., McIntyre, D., Shen, Y., O'Sullivan, M., Howe, F., Clark, C., Morris, R., Markus, H., 2006. White matter damage on diffusion tensor imaging correlates with age-related cognitive decline. Neurology 66, 217–222.
Chee, M.W., Chen, K.H., Zheng, H., Chan, K.P., Isaac, V., Sim, S.K., Chuah, L.Y., Schuchinsky, M., Fischl, B., Ng, T.P., 2009. Cognitive function and brain structure correlations in healthy elderly East Asians. NeuroImage 46, 257–269.
Cortese, S., Imperati, D., Zhou, J., Proal, E., Klein, R.G., Mannuzza, S., Ramos-Olazagasti, M.A., Milham, M.P., Kelly, C., Castellanos, F.X., 2013. White matter alterations at 33-Year follow-up in adults with childhood attention-deficit/hyperactivity disorder. Biol. Psychiatry 74, 591–598.
Daye, Z.J., Xie, J., Li, H., 2012. A sparse structured shrinkage estimator for nonparametric varying-coefficient model with an application in genomics. J. Comput. Graph. Stat. 21, 110–133.
DeLong, M., Alexander, G., Georgopoulos, A., Crutcher, M., Mitchell, S., Richardson, R., 1984. Role of basal ganglia in limb movements. Hum. Neurobiol. 2, 235.
Eckert, M.A., Keren, N.I., Roberts, D.R., Calhoun, V.D., Harris, K.C., 2010. Age-related changes in processing speed: unique contributions of cerebellar and prefrontal cortex. Front. Hum. Neurosci. 4, 1–14.
Ell, S.W., Helie, S., Hutchinson, S., 2011. Contributions of the putamen to cognitive function. In: Costa, A., Villalba, E. (Eds.), Horizon in Neuroscience. Nova Publishers.
Fjell, A.M., Walhovd, K.B., 2010. Structural brain changes in aging: courses, causes and cognitive consequences. Rev. Neurosci. 21, 187–221.
Folstein, M.F., Folstein, S.E., McHugh, P.R., 1975. "Mini-mental state": a practical method for grading the cognitive state of patients for the clinician. J. Psychiatr. Res. 12, 189–198.
Giorgio, A., Santelli, L., Tomassini, V., Bosnell, R., Smith, S., De Stefano, N., Johansen-Berg, H., 2010. Age-related changes in grey and white matter structure throughout adulthood. NeuroImage 51, 943–951.
Good, C.D., Johnsrude, I.S., Ashburner, J., Henson, R.N., Friston, K.J., Frackowiak, R.S., 2001. A voxel-based morphometric study of ageing in 465 normal adult human brains. NeuroImage 14, 21–36.
Haasz, J., Westlye, E.T., Fjaer, S., Espeseth, T., Lundervold, A., Lundervold, A.J., 2013. General fluid-type intelligence is related to indices of white matter structure in middle-aged and old adults. NeuroImage 83, 372–383.
Haber, S.N., 2010. Integrative networks across basal ganglia circuits. In: Steiner, H., Tseng, K.Y. (Eds.), Handbook of Basal Ganglia Structure and Function. Elsevier, Oxford.
Hayasaka, S., Nichols, T.E., 2004. Combining voxel intensity and cluster extent with permutation test framework. NeuroImage 23, 54–63.
Hayes, A.F., 2009. Beyond Baron and Kenny: statistical mediation analysis in the new millennium. Commun. Monogr. 76, 408–420.
Imperati, D., Colcombe, S., Kelly, C., Di Martino, A., Zhou, J., Castellanos, F.X., Milham, M.P., 2011. Differential development of human brain white matter tracts. PLoS One 6, e23437.
Jacobs, H.I., Leritz, E.C., Williams, V.J., Van Boxtel, M.P., Elst, W., Jolles, J., Verhey, F.R., McGlinchey, R.E., Milberg, W.P., Salat, D.H., 2013. Association between white matter microstructure, executive functions, and processing speed in older adults: the impact of vascular health. Hum. Brain Mapp. 34, 77–95.
Jernigan, T.L., Archibald, S.L., Fennema-Notestine, C., Gamst, A.C., Stout, J.C., Bonner, J., Hesselink, J.R., 2001. Effects of age on tissues and regions of the cerebrum and cerebellum. Neurobiol. Aging 22, 581–594.
Kalpouzos, G., Chetelat, G., Baron, J.C., Landeau, B., Mevel, K., Godeau, C., Barre, L., Constans, J.M., Viader, F., Eustache, F., Desgranges, B., 2009. Voxel-based mapping of brain gray matter volume and glucose metabolism profiles in normal aging. Neurobiol. Aging 30, 112–124.
Kennedy, K.M., Raz, N., 2009a. Aging white matter and cognition: differential effects of regional variations in diffusion properties on memory, executive functions, and speed. Neuropsychologia 47, 916–927.
Kennedy, K.M., Raz, N., 2009b. Pattern of normal age-related regional differences in white matter microstructure is modified by vascular risk. Brain Res. 1297, 41–56.
Kennedy, K.M., Erickson, K.I., Rodrigue, K.M., Voss, M.W., Colcombe, S.J., Kramer, A.F., Acker, J.D., Raz, N., 2009. Age-related differences in regional brain volumes: a comparison of optimized voxel-based morphometry to manual volumetry. Neurobiol. Aging 30, 1657–1676.
Kerchner, G.A., Racine, C.A., Hale, S., Wilheim, R., Laluz, V., Miller, B.L., Kramer, J.H., 2012. Cognitive processing speed in older adults: relationship with white matter integrity. PLoS One 7, e50425.
Kochunov, P., Glahn, D.C., Lancaster, J., Thompson, P.M., Kochunov, V., Rogers, B., Fox, P., Blangero, J., Williamson, D.E., 2011. Fractional anisotropy of cerebral white matter and thickness of cortical gray matter across the lifespan. NeuroImage 58, 41–49.
Lebel, C., Gee, M., Camicioli, R., Wieler, M., Martin, W., Beaulieu, C., 2012. Diffusion tensor imaging of white matter tract evolution over the lifespan. NeuroImage 60, 340–352.
Lindenberger, U., von Oertzen, T., Ghisletta, P., Hertzog, C., 2011. Cross-sectional age variance extraction: what's change got to do with it? Psychol. Aging 26, 34–47.
Lovden, M., Kohncke, Y., Laukka, E.J., Kalpouzos, G., Salami, A., Li, T.Q., Fratiglioni, L., Backman, L., 2014. Changes in perceptual speed and white matter microstructure in the corticospinal tract are associated in very old age. NeuroImage 102 (Pt 2), 520–530.
Lu, P.H., Lee, G.J., Raven, E.P., Tingus, K., Khoo, T., Thompson, P.M., Bartzokis, G., 2011. Age-related slowing in cognitive processing speed is associated with myelin integrity in a very healthy elderly sample. J. Clin. Exp. Neuropsychol. 33, 1059–1068.
Madden, D.J., Whiting, W.L., Huettel, S.A., White, L.E., MacFall, J.R., Provenzale, J.M., 2004. Diffusion tensor imaging of adult age differences in cerebral white matter: relation to response time. NeuroImage 21, 1174–1181.
Madden, D.J., Bennett, I.J., Song, A.W., 2009. Cerebral white matter integrity and cognitive aging: contributions from diffusion tensor imaging. Neuropsychol. Rev. 19, 415–435.
Madden, D.J., Bennett, I.J., Burzynska, A., Potter, G.G., Chen, N.K., Song, A.W., 2012. Diffusion tensor imaging of cerebral white matter integrity in cognitive aging. Biochim. Biophys. Acta 1822, 386–400.
Marchand, W.R., Lee, J.N., Thatcher, J.W., Hsu, E.W., Rashkin, E., Suchy, Y., Chelune, G., Starr, J., Barbera, S.S., 2008. Putamen coactivation during motor task execution. Neuroreport 19, 957–960.
Maxwell, S.E., Cole, D.A., 2007. Bias in cross-sectional analyses of longitudinal mediation. Psychol. Methods 12, 23–44.
Mori, S., Wakana, S., Van Zijl, P.C.M., Nagae-Poetscher, L.M., 2005. MRI atlas of human white matter. Elsevier, Amsterdam, The Netherlands.
O'Sullivan, M., Jones, D., Summers, P., Morris, R., Williams, S., Markus, H., 2001. Evidence for cortical "disconnection" as a mechanism of age-related cognitive decline. Neurology 57, 632–638.
Ostby, Y., Tamnes, C.K., Fjell, A.M., Westlye, L.T., Due-Tonnessen, P., Walhovd, K.B., 2009. Heterogeneity in subcortical brain development: a structural magnetic resonance imaging study of brain maturation from 8 to 30 years. J. Neurosci. Off. J. Soc. Neurosci. 29, 11772–11782.
Pfefferbaum, A., Sullivan, E.V., Hedehus, M., Lim, K.O., Adalsteinsson, E., Moseley, M., 2000. Age-related decline in brain white matter anisotropy measured with spatially corrected echo-planar diffusion tensor imaging. Magn. Reson. Med. 44, 259–268.
Pfefferbaum, A., Adalsteinsson, E., Sullivan, E.V., 2005. Frontal circuitry degradation marks healthy adult aging: evidence from diffusion tensor imaging. NeuroImage 26, 891.
Rao, S.M., Mayer, A.R., Harrington, D.L., 2001. The evolution of brain activation during temporal processing. Nat. Neurosci. 4, 317–323.
Reitan, R.M., Wolfson, D., 1985. The Halstead-Reitan Neuropsychological Test Battery. Neuropsychology Press, Tucson, Ariz.
Righart, R., Duering, M., Gonik, M., Jouvent, E., Reyes, S., Hervé, D., Chabriat, H., Dichgans, M., 2013. Impact of regional cortical and subcortical changes on processing speed in cerebral small vessel disease. NeuroImage 2, 854–861.
Salami, A., Eriksson, J., Nilsson, L.G., Nyberg, L., 2012. Age-related white matter microstructural differences partly mediate age-related decline in processing speed but not cognition. Biochim. Biophys. Acta 1822, 408–415.
Salthouse, T.A., 1995. Processing capacity and its role on the relations between age and memory. Memory performance and competencies: Issues in growth and development pp. 111–126.
Salthouse, T.A., 2000. Aging and measures of processing speed. Biol. Psychol. 54, 35–54.
Salthouse, T.A., 2009. When does age-related cognitive decline begin? Neurobiol. Aging 30, 507–514.
Salthouse, T.A., 2010. Selective review of cognitive aging. J. Int. Neuropsychol. Soc. 16, 754–760.
Salthouse, T.A., 2011. Neuroanatomical substrates of age-related cognitive decline. Psychol. Bull. 137, 753–784.
Salthouse, T.A., Ferrer-Caja, E., 2003. What needs to be explained to account for age-related effects on multiple cognitive variables? Psychol. Aging 18, 91–110.
Schubotz, R.I., Friederici, A.D., von Cramon, D.Y., 2000. Time perception and motor timing: a common cortical and subcortical basis revealed by fMRI. NeuroImage 11, 1–12.
Shaw, P., Kabani, N.J., Lerch, J.P., Eckstrand, K., Lenroot, R., Gogtay, N., Greenstein, D., Clasen, L., Evans, A., Rapoport, J.L., Giedd, J.N., Wise, S.P., 2008. Neurodevelopmental trajectories of the human cerebral cortex. J. Neurosci. Off. J. Soc. Neurosci. 28, 3586–3594.
Sheikh, J.I., Yesavage, J.A., 1986. Geriatric Depression Scale (GDS): recent evidence and development of a shorter version. Clin. Gerontol. 5, 165–173.
Shenkin, S.D., Bastin, M.E., Macgillivray, T.J., Deary, I.J., Starr, J.M., Rivers, C.S., Wardlaw, J.M., 2005. Cognitive correlates of cerebral white matter lesions and water diffusion tensor parameters in community-dwelling older people. Cerebrovasc. Dis. 20, 310–318.
Smith, A., 1991. Symbol Digit Modalities Test. Western Psychological Services, Los Angeles, C.A.
Smith, S.M., Nichols, T.E., 2009. Threshold-free cluster enhancement: addressing problems of smoothing, threshold dependence and localisation in cluster inference. NeuroImage 44, 83–98.
Smith, S.M., Jenkinson, M., Johansen-Berg, H., Rueckert, D., Nichols, T.E., Mackay, C.E., Watkins, K.E., Ciccarelli, O., Cader, M.Z., Matthews, P.M., 2006. Tract-based spatial statistics: voxelwise analysis of multi-subject diffusion data. NeuroImage 31, 1487–1505.
Sowell, E.R., Peterson, B.S., Thompson, P.M., Welcome, S.E., Henkenius, A.L., Toga, A.W., 2003. Mapping cortical change across the human life span. Nat. Neurosci. 6, 309–315.
Sullivan, E.V., Pfefferbaum, A., 2006. Diffusion tensor imaging and aging. Neurosci. Biobehav. Rev. 30, 749–761.
Sullivan, E.V., Rohlfing, T., Pfefferbaum, A., 2010. Quantitative fiber tracking of lateral and interhemispheric white matter systems in normal aging: relations to timed performance. Neurobiol. Aging 31, 464–481.
Tibshirani, R., 1996. Regression shrinkage and selection via the lasso. J. R. Stat. Soc. Ser. B Methodol. 267–288.
Turner, R.S., Desmurget, M., Grethe, J., Crutcher, M.D., Grafton, S.T., 2003. Motor subcircuits mediating the control of movement extent and speed. J. Neurophysiol. 90, 3958–3966.

Vernooij, M.W., Ikram, M.A., Vrooman, H.A., Wielopolski, P.A., Krestin, G.P., Hofman, A., Niessen, W.J., Van der Lugt, A., Breteler, M., 2009. White matter microstructural integrity and cognitive function in a general elderly population. Arch. Gen. Psychiatry 66, 545.

Voineskos, A.N., Rajji, T.K., Lobaugh, N.J., Miranda, D., Shenton, M.E., Kennedy, J.L., Pollock, B.G., Mulsant, B.H., 2012. Age-related decline in white matter tract integrity and cognitive performance: a DTI tractography and structural equation modeling study. Neurobiol. Aging 33, 21–34.

Wakana, S., Jiang, H., Nagae-Poetscher, L.M., Van Zijl, P.C., Mori, S., 2004. Fiber tract–based atlas of human white matter anatomy. Radiology 230, 77–87.

Walhovd, K.B., Fjell, A.M., Reinvang, I., Lundervold, A., Dale, A.M., Eilertsen, D.E., Quinn, B.T., Salat, D., Makris, N., Fischl, B., 2005. Effects of age on volumes of cortex, white matter and subcortical structures. Neurobiol. Aging 26, 1261–1270 (discussion 1275–1268).

Walhovd, K.B., Westlye, L.T., Amlien, I., Espeseth, T., Reinvang, I., Raz, N., Agartz, I., Salat, D.H., Greve, D.N., Fischl, B., Dale, A.M., Fjell, A.M., 2011. Consistent neuroanatomical age-related volume differences across multiple samples. Neurobiol. Aging 32, 916–932.

Wechsler, D., 1997. WMS-III Administration and Scoring Manual. The Psychological Corporation, San Antonio, Tex.

Westlye, L.T., Walhovd, K.B., Dale, A.M., Bjornerud, A., Due-Tonnessen, P., Engvig, A., Grydeland, H., Tamnes, C.K., Ostby, Y., Fjell, A.M., 2010. Life-span changes of the human brain white matter: diffusion tensor imaging (DTI) and volumetry. Cereb. Cortex 20, 2055–2068.

Ystad, M., Hodneland, E., Adolfsdottir, S., Haasz, J., Lundervold, A.J., Eichele, T., Lundervold, A., 2011. Cortico-striatal connectivity and cognition in normal aging: a combined DTI and resting state fMRI study. NeuroImage 55, 24–31.

Zahr, N.M., Rohlfing, T., Pfefferbaum, A., Sullivan, E.V., 2009. Problem solving, working memory, and motor correlates of association and commissural fiber bundles in normal aging: a quantitative fiber tracking study. NeuroImage 44, 1050–1062.

Zhang, H., Sachdev, P.S., Wen, W., Kochan, N.A., Zhu, W., Crawford, J.D., Brodaty, H., Slavin, M.J., Reppermund, S., Kang, K., 2011. Neuroanatomical correlates of cognitive performance in late life. Dement. Geriatr. Cogn. Disord. 32, 216–226.

Zhou, J., Greicius, M.D., Gennatas, E.D., Growdon, M.E., Jang, J.Y., Rabinovici, G.D., Kramer, J.H., Weiner, M., Miller, B.L., Seeley, W.W., 2010. Divergent network connectivity changes in behavioural variant frontotemporal dementia and Alzheimer's disease. Brain 133, 1352–1367.